

The light curve of the semiregular variable L₂ Puppis: I. A recent dimming event from dust

T. R. Bedding,^{1*} A.A. Zijlstra,² A. Jones³, F. Marang⁴, M. Matsuura², A. Retter¹, P.A. Whitelock⁴ and I. Yamamura⁵

¹*School of Physics, University of Sydney 2006, Australia*

²*UMIST, Department of Physics, P.O. Box 88, Manchester M60 1QD, UK*

³*Carter Observatory, P.O. Box 2909, Wellington, New Zealand*

⁴*SAAO, P.O. Box 9, Observatory 7935, South Africa*

⁵*The Institute of Space and Astronautical Science, 3-1-1 Yoshino-dai, Sagamihara, 299-8510, Kanagawa, Japan*

26 October 2018

ABSTRACT

The nearby Mira-like variable L₂ Pup is shown to be undergoing an unprecedented dimming episode. The stability of the period rules out intrinsic changes to the star, leaving dust formation along the line of sight as the most likely explanation. Episodic dust obscuration events are fairly common in carbon stars but have not been seen in oxygen-rich stars. We also present a 10- μ m spectrum, taken with the Japanese IRTS satellite, showing strong silicate emission which can be fitted with a detached, thin dust shell, containing silicates and corundum.

Key words: stars: individual: L₂ Pup – stars: AGB and post-AGB – stars: oscillations – stars: mass-loss – stars: variables: other

1 INTRODUCTION

L₂ Puppis (HR 2748; HIP 34922) is a bright nearby red giant with a pulsation period of about 140 d. Its spectral type of M5eIII and luminosity of 1500 L_⊙ indicate that it is evolving towards the tip of the Asymptotic Giant Branch (AGB). Evidence for mass loss at a rate of $3 \times 10^{-7} M_{\odot} \text{ yr}^{-1}$ (Jura et al. 2002) supports this. L₂ Pup is possibly the nearest star in this evolutionary phase, at a Hipparcos distance of 61 ± 5 pc. Among known long-period AGB stars, only R Doradus has a similar distance. At 12 microns, L₂ Pup is among the 15 brightest sources in the IRAS point source catalogue.

L₂ Pup is unusual in several respects. Firstly, it shows a high degree of optical polarization, with a variable wavelength dependence that implies a long timescale for the growth and dissipation of dust grains (of the order of a decade; Magalhaes et al. 1986). Secondly, CO measurements by Kerschbaum & Olofsson (1999) indicate a very low expansion velocity (about 2.5 km s⁻¹), which led them to label L₂ Pup as an extreme case, with one of the smallest expansion velocities ever measured for an AGB star. The slow wind from L₂ Pup led Winters et al. (2000, 2002) to suggest that this star could represent their B-model, in which mass loss is driven entirely by pulsations, without any significant input from radiation pressure on dust grains. This has been further discussed by Jura et al. (2002), who modelled the mass loss and suggested that the pulsations may be non-radial.

Thirdly, as we report here, this star has shown a remarkable change in mean visual magnitude over the past century, and is currently undergoing a dramatic dimming. We present visual and infrared photometry which characterizes this behaviour, and argue that the most likely cause is the formation of dust along the line of sight. We also present the first 10-micron spectrum of L₂ Pup, obtained with the Japanese IRTS satellite, which shows strong silicate emission.

2 LIGHT CURVE

2.1 Visual observations

We have analysed visual observations of L₂ Pup from the following sources: the Royal Astronomical Society of New Zealand (RASNZ; 12100 measurements by 110 observers, including 1100 by A. Jones), the Variable Star Observers League in Japan (VSOLJ; 792 measurements by 6 observers) and the Association Francaise des Observateurs d’Etoiles Variables (AFOEV; 389 measurements by 3 observers). Only data from individual observers contributing 30 or more observations were used and we did not attempt to correct for offsets between observers. The top panel of Fig. 1 shows the combined data, binned to 10-day averages.

The variation in mean magnitude is evident. Before 1945 the data are too patchy and/or noisy to reach strong conclusions. However, it is clear that the star faded significantly after 1960, recovering around 1975 but remaining fainter by about 0.5 mag compared

* E-mail: bedding@physics.usyd.edu.au

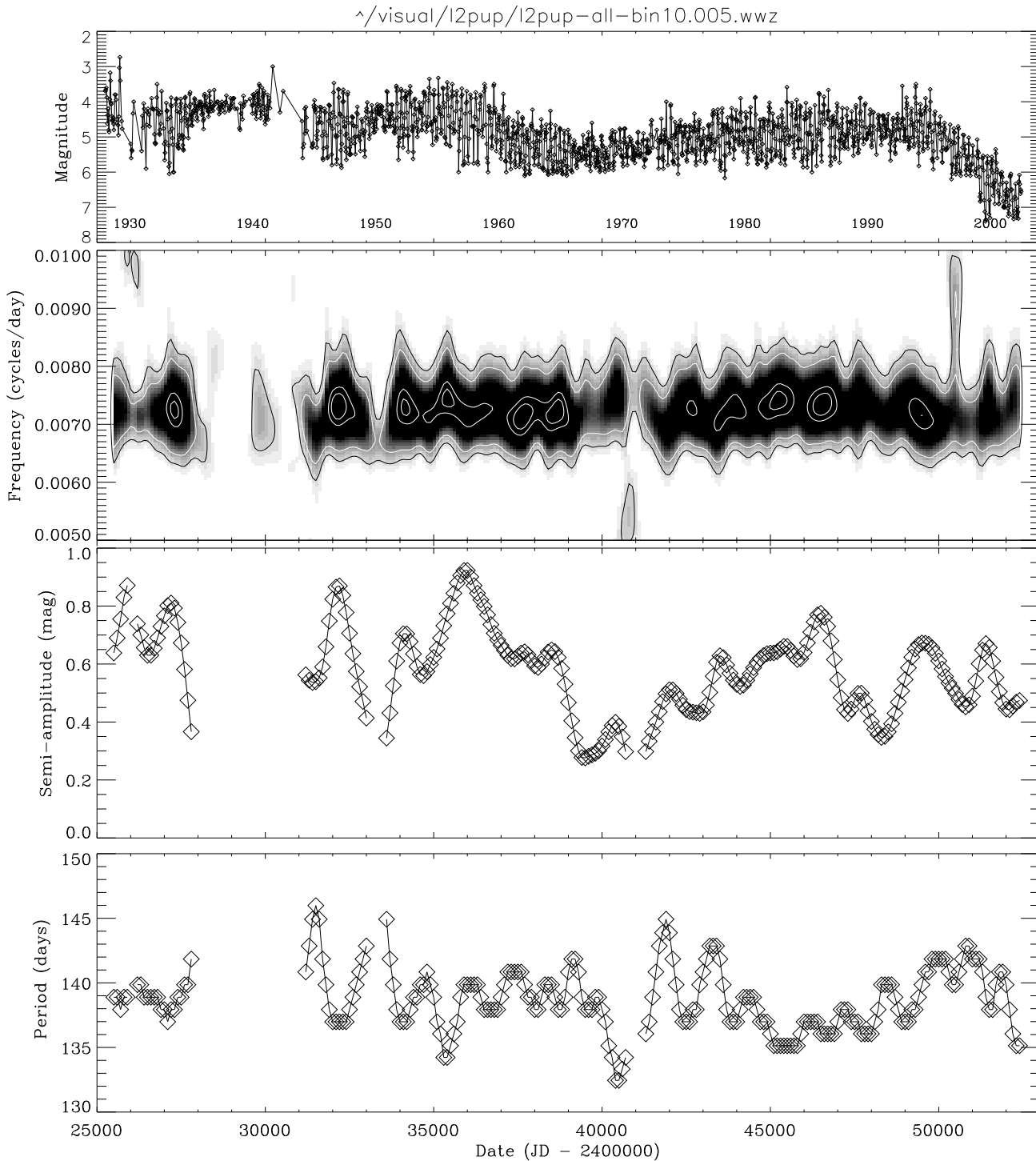


Figure 1. Wavelet analysis for L_2 Pup. Top to bottom: the light curve (in 10-day bins), the WWZ transform, the semi-amplitude and the period.

to the 1950s. Recently, starting around 1994, a dramatic fading has occurred. Even at maximum, the star now remains fainter than magnitude 6, and it is no longer a naked-eye variable.

We have used wavelet analysis to search for period and amplitude changes. Wavelets have been used previously to study long-period variables (e.g., Szatmáry et al. 1996; Bedding et al. 1998; Kiss et al. 1999). We used the weighted wavelet Z-transform

(WWZ; Foster 1996), developed specifically for unevenly sampled data. We experimented with different values for the parameter c , which defines the tradeoff between time resolution and frequency resolution Foster (1996), and settled on $c = 0.005$ as a good compromise. More details of the application of the WWZ transform to long-period variables are given by Bedding et al. (1998).

The lower three panels of Figure 1 show the wavelet plots for

L₂ Pup, based on the light curve in the top panel. The second panel shows the WWZ transform, with the grey scale indicating the significance of each frequency as a function of time (see Bedding et al. 1998). Only a small range of frequencies is shown – there is no evidence for significant power outside this range. The third and fourth panels show, for each time bin, the semi-amplitude (in magnitudes) and period (in days) corresponding to the peak of the WWZ in the second panel.

It is clear from Fig. 1 that the period of L₂ Pup has remained within a fairly narrow range (135–145 d) for the past 75 years. Such period jitter is common among semiregular and Mira variables. There is a slight indication of a lengthening of period *before* the onset of the recent dimming, from 136 to 142 days, but the change (at most 4%) is well within the range of normal Mira variables. The amplitude, on the other hand, has changed significantly over the years, but the changes are apparently uncorrelated with the period jitter.

L₂ Pup is classified as an SRb variable, a class of stars with poorly defined periodicity. In fact, the period of this star is remarkably stable. The characteristics of the wavelet plot show that L₂ Pup should be classified as SRa, a class closely related to Miras, often differing only in having smaller amplitudes.

2.2 Early observations

L₂ Pup was discovered to be variable by Gould in 1872 (Cannon & Pickering 1907). Roberts (1893) estimated a period of 137.2 d from the dates of nine maxima observed by himself, Gould and Williams during 1872–92. Cannon & Pickering (1907), in the *Second Catalogue of Variable Stars*, quoted a period of 140.15 d, which they attributed to Roberts. Cannon & Pickering (1909) listed dates of maxima going back to 1872, and also adopted a period of 140.15 d. It therefore seems that the period of L₂ Pup has remained within a narrow range since its discovery.

The visual magnitude at maximum during the late 1800s was about 3.6 (Williams 1897; Cannon & Pickering 1909), consistent with modern (1950s) out-of-decline values. Müller & Hartwig (1922) listed the magnitude range since discovery as 3.4–4.6 at maximum and 5.8–6.2 at minimum. This suggests that, between 1872 and 1918, L₂ Pup was never as faint as it currently is.

2.3 Near-infrared photometry

We have taken *JHKL* infrared photometry from Whitelock et al. (2000), together with more recent observations obtained with the same system (see Table 1). The infrared observations are much less frequent than the visual ones and do not sample the pulsation cycle very well. Nevertheless, the mean infrared magnitudes can be estimated, and we have shown these in Fig. 2 by fitting a low-order polynomial to each waveband.

The dimming at *V* is followed at all infrared bands, although with reduced amplitude. The *J* – *K* colour has reddened during the dimming.

The mean *K* magnitude before the dimming was –2.34 (Table 4 of Whitelock et al. 2000). More recently, the magnitude dropped to –2.0 or fainter¹. The Hipparcos distance allows comparison with the *K*-band period–luminosity (P–L) relation for nearby Miras (Whitelock & Feast 2000):

¹ Bedding & Zijlstra (1998) gave *K* = –2.65, but this was a transcription error and should have read –2.15.

Table 1. Near-infrared photometry of L₂ Pup

JD – 2400000	<i>J</i>	<i>H</i>	<i>K</i>	<i>L</i>
51186	–0.865	–1.833	–2.276	–2.889
51239	–0.273	–1.200	–1.792	–2.594
51574	–1.013	–1.968	–2.375	–2.958
51599	–0.976	–1.941	–2.369	–2.972
51613	–0.918	–1.902	–2.352	–2.901
51858	–0.796	–1.753	–2.201	–2.901
51868	–0.775	–1.742	–2.199	–2.823
51887	–0.691	–1.695	–2.178	–2.834
51928	–0.118	–1.130	–1.720	–2.538
51962	–0.645	–1.536	–1.998	–2.708
51979	–0.783	–1.696	–2.101	–2.676
52181	–0.562	–1.614	–2.106	–2.730
52242	–0.601	–1.497	–1.964	–2.632
52258	–0.877	–1.764	–2.138	–2.776

Table 2. Pre-dimming and present mean magnitudes and colours of L₂ Pup

	pre-dimming	present
<i>V</i>	4.8	6.8
<i>J</i>	–1.03	–0.25
<i>H</i>	–1.94	–1.25
<i>K</i>	–2.34	–1.8
<i>L</i>	–2.91	–2.7
<i>V</i> – <i>K</i>	7.0	8.5
<i>J</i> – <i>K</i>	1.31	1.55
<i>m</i> _{bol}	0.73 ^a	1.3 ^a

^a assuming no extinction correction

$$M_K = -3.47 \log P + 0.84. \quad (1)$$

For L₂ Pup, this relation predicts $M_K = -6.64$, which compares relatively poorly to the observed value of $M_K = -6.16$. The recent fading has worsened the agreement. Thus, L₂ Pup appears to be one of a small fraction of stars located below the P–L relation. We will return to this in Sec. 3.3.

Table 2 shows the mean colours and magnitudes before and after the dimming. The pre-dimming NIR magnitudes are taken from Table 4 of Whitelock et al. (2000). The current values are derived from the fits in Fig. 2, and are somewhat more uncertain because of the poor sampling of the pulsation cycle.

3 DISCUSSION OF THE DIMMING

What causes the large variations in mean magnitude of L₂ Pup, especially the current dramatic fading? We consider three possibilities: changes in temperature, luminosity and extinction.

3.1 Change in stellar temperature and/or luminosity

In late M-type giants, the optical flux is very sensitive to temperature. Even a slight cooling would lead to a sharp drop in *V* via the formation of temperature-sensitive molecules (TiO, VO) that absorb strongly at optical wavelengths (Reid & Goldston 2002).

We first need to estimate the effective temperature of L₂ Pup. In the absence of a measured angular diameter, this requires reference to published temperature scales. The temperature scales for

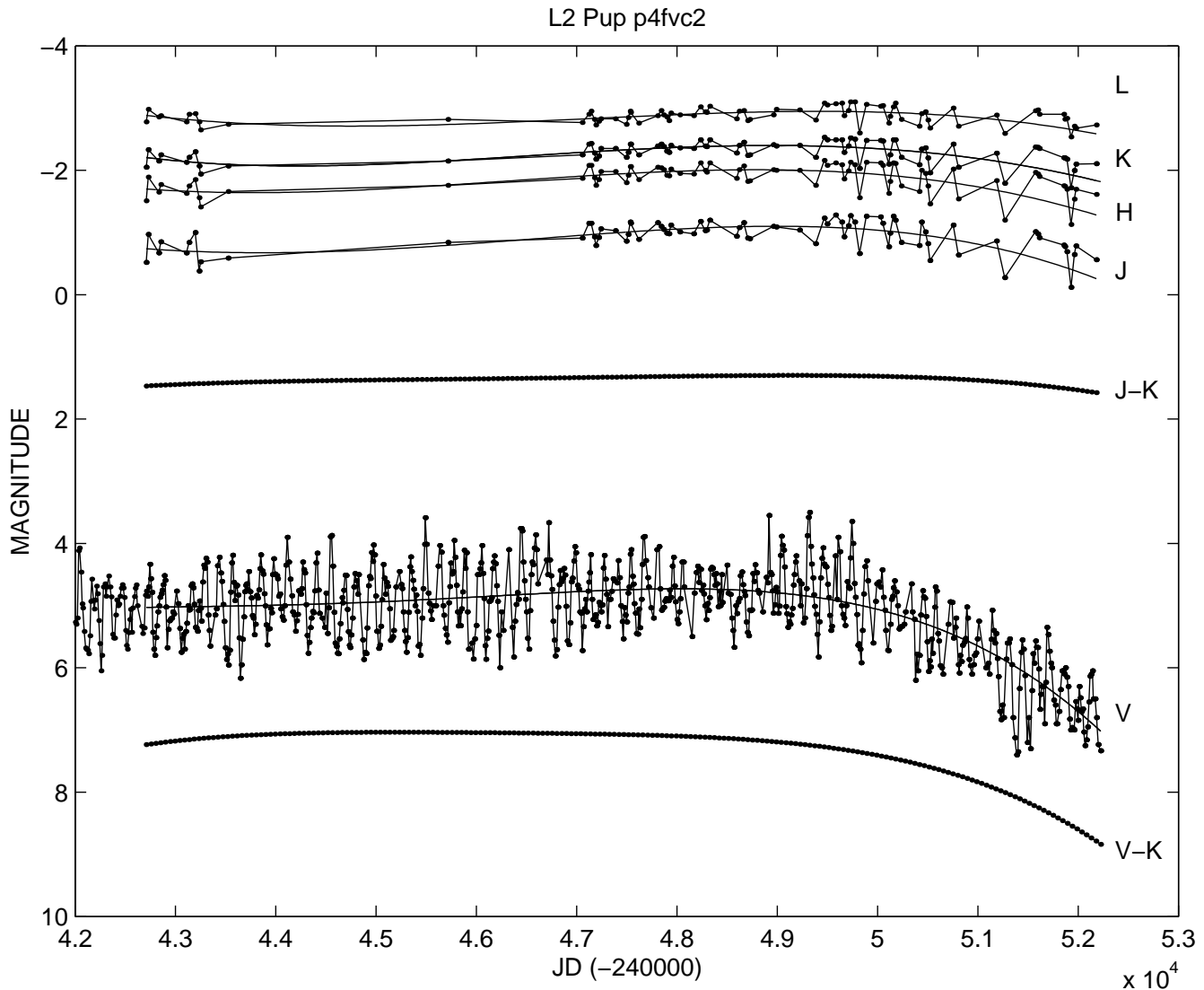


Figure 2. Infrared and visual photometry for L_2 Pup.

M-giants differ greatly for stars with and without extended atmospheres. Assuming no extended atmosphere, the pre-dimming $V - K$ colour index of L_2 Pup implies $T_{\text{eff}} \approx 3200$ K (Bessell et al. 1998; Houdashelt et al. 2000). Models with this temperature also give a $J - K$ colour consistent with the observed value. Jura et al. (2002) adopted a temperature of 3400 K, also taken from photospheric models, which is also consistent with the scale of van Belle et al. (1996).

However, stars with extended atmospheres have much lower colour temperatures (Feast 1996; van Belle et al. 2002). The following relation was given by Feast (1996) for Miras, based on interferometric angular diameters:

$$\log T_{\text{eff}} = -0.474(J - K)_0 + 4.059. \quad (2)$$

For L_2 Pup, the pre-dimming $J - K$ colour index yields the much lower value of $T_{\text{eff}} = 2775$ K. Since this star is Mira-like and shows evidence for mass loss, the atmosphere is likely to be extended and the lower temperature is probably a better description of its optical/NIR spectral energy distribution.

During the fading, $J - K$ increased to 1.55, which corresponds

to a temperature decline of 660 K on the scale of Feast (1996). The increase in $V - K$ to 8.5, would correspond to a temperature decline of about 300 K in the Bessell et al. (1998) models. The bolometric correction, BC_K , increased from 3.05 to 3.21 on the low-temperature scale, and from 3.05 to 3.15 on the high temperature scale (Whitelock et al. 2000; Bessell et al. 1998). The luminosity decline in either case is about a factor of 1.8. Using $L \propto R^2 T_{\text{eff}}^4$, we conclude that the radius would have decreased by 10% on the high-T scale and increased by 20% on the low-T scale.

Such large changes in radius can be ruled out because of the stable period. The maximum period change allowed by the observations is about 6% (see Fig. 1). Since the period of a pulsating star scales inversely with the square root of stellar density, we can infer that the radius cannot have changed by more than 4% (since $P \propto R^{3/2}$). In fact, we can take the relative stability of the pulsation period over the past 130 years to be evidence that the density of the star has not changed significantly. The period variations that are observed in L_2 Pup are similar to those seen in many semiregular variables and are most likely due to the influence on the pulsation driving by random convective excitation (Christensen-Dalsgaard

et al. 2001). We discuss this in more detail in Paper II (Bedding et al. 2002).

The period is stable on the same timescales over which the mean magnitude is variable, which argues that radius changes cannot be part of the explanation of the dimming. If we assume a constant radius, we could still produce the observed change in m_{bol} if the temperature decreased by about 400 K. Such a temperature change cannot be ruled out but would require fine tuning. Furthermore, such a large change in stellar luminosity over a time scale of a decade only occurs in AGB stars in the immediate aftermath of a thermal pulse. Finding any star in such a short-lived phase is very unlikely. In any case, the thermal-pulse scenario can also be ruled out because, during this phase, the radius strongly contracts and the period shortens (e.g. Vassiliadis & Wood 1993), which is not observed in L_2 Pup.

It is therefore unlikely that either the radius or the luminosity of the star has changed. This points towards variable extinction as the cause of the dimming.

3.2 Extinction from circumstellar dust

The plausible cause of the fading in L_2 Pup is extinction by circumstellar dust, which would not affect the amplitude or period of pulsation of the underlying star. Extinction laws for interstellar dust are well studied and predict less extinction as one moves to longer wavelengths. This is certainly the case for L_2 Pup, as can be seen from Fig. 2: the decline is much less dramatic in $JHKL$ than in V .

Direct evidence for extinction comes from the present $J - K$ and $K - L$, which are among the reddest of the M-type variables in the sample of Whitelock et al. (2000). All stars with such red colours have K -band amplitudes larger than 0.7 mag, while the amplitude for L_2 Pup is only 0.29 mag at K . In fact, both ΔK and δH_p (0.71) are small compared to M-type variables. This large discrepancy between colour and amplitude suggests that the red colours are partly caused by extinction.

L_2 Pup is also anomalously red for its period. The average relation between colour and period for Miras is

$$J - K = -0.39 \pm 0.15 + (0.71 \pm 0.06) \log P, \quad (3)$$

(Whitelock et al. 2000). For L_2 Pup, this relation predicts $J - K = 1.13$, compared with 1.31 pre-dimming and 1.55 at present. The observed values suggest that significant extinction existed even before the present dimming. Assuming a linear relation between the $J - K$ excess and the visual extinction, and assuming that the post-1995 dimming of 2 mag at V and 0.24 in $J - K$ is due to extinction, the pre-dimming $J - K$ excess of 0.18 would correspond to a visual extinction of about 1.5 mag at V .

This estimate suggests that the long-term V -band variations may be due to variable extinction. The brightest epoch, in the 1950s, could in this case give the best indication of the unreddened magnitude. However, while L_2 Pup is Mira-like in some properties, it is certainly not a true Mira and so results based on applying Eq. 3 should be treated with some caution.

3.3 Extinction curve and the Mira P-L relation

Typical extinction constants for interstellar dust are listed in Bessell et al. (1998). For the observed post-1995 $J - K$ reddening, they give $\Delta A_K = 0.15$. This is less than half the decline at K shown in Fig. 2, suggesting this extinction curve is too steep. To investigate this quantitatively, we show in Fig. 3 the locus (M, V) of the mean

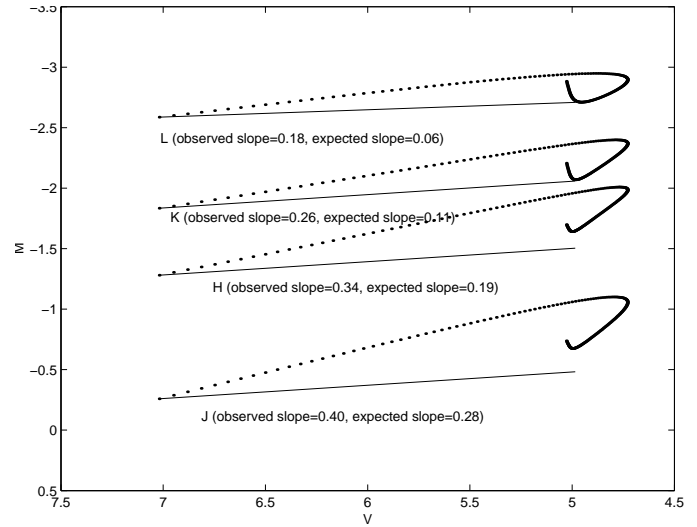


Figure 3. Infrared versus V photometry for L_2 Pup, using the polynomial fits shown in Fig. 2. The vertical axis is the infrared magnitude, for $M = J, H, K, L$. Written on each plot are the observed slope and the expected slopes, the latter taken from Table 3 of (Cardelli et al. 1989).

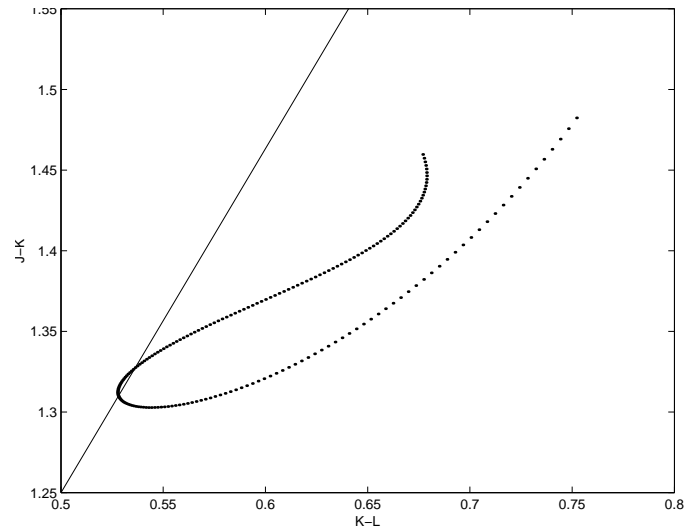


Figure 4. Infrared colour-colour diagram of L_2 Pup, using the polynomial fits shown in Fig. 2. The diagonal line shows the interstellar reddening vector, with $A_V = 1.0$, $E(J - K) = 0.164$ and $E(K - L) = 0.045$.

infrared magnitude versus the V magnitude, for $M = J, H, K, L$. Also shown are straight lines with slopes taken from Table 3 of Cardelli et al. (1989), which are standard values for extinction by interstellar dust. We can see that the observed slopes are in all cases larger than expected, and the discrepancy is progressively greater at longer wavelengths. The interstellar extinction curve appears inappropriate: instead the extinction appears to be ‘greyer.’ This could be due to a contribution from oxides, which can form at high temperatures (Henning 1996). The infrared colour-colour diagram, shown in Fig. 4, confirms that the reddening is less steep than expected from interstellar extinction.

The colour differential suggests that $A_K/A_V \approx 0.3$. If we assume that the pre-dimming (1995) extinction at V was $A_V \approx 1.5$ mag, the K -band would already have been affected by 0.5 mag, so that $M_{K,0} \approx -6.7$. This is close to the value expected from the

Mira P–L relation, and well within the $1\text{-}\sigma$ uncertainty contributed by the error on the Hipparcos parallax. It therefore appears possible that the Mira P–L relation is an accurate indicator of the de-reddened magnitude of L₂ Pup.

3.4 Dust location

For a pulsation velocity of 3 km s^{-1} , the gas travels at most $1R_*$ per year. The short timescale of the dimming thus suggests that the new dust is located within a few stellar radii of the star, possibly less. The rapid variation in polarization angle (Magalhaes et al. 1986) also suggests that dust forms close to the star. The timescale for dust formation derived by these authors based on the polarization (about a decade) is consistent with the timescale of extinction variations.

The polarization shows that the dust is not distributed isotropically, and the variation in polarization angle shows that the distribution is not constant. Dust may form continuously, but in different directions: the present dimming event would, in that case, correspond to dust formation along the line of sight.

3.5 Extinction episodes in other Mira variables

Dimming episodes lasting a number of pulsation cycles (decades) are seen in carbon Miras, with similarities to the dust obscuration events of R CrB stars (Percy et al. 1990). Lloyd Evans (1997) found that these episodes are accompanied by strong emission in the Swan C₂ band 5165 \AA , while Whitelock et al. (1997) found them to occur in carbon stars with thick circumstellar envelopes.

Could the fading of the non-carbon star L₂ Pup be a related phenomenon? Lloyd Evans (1997) listed five Miras with dust fadings which probably have relatively low C/O ratios (W Aql, U Cyg, Y Del, S Lyr and RU Vir), and Whitelock et al. (2000) added Y Vel to this list. Unlike L₂ Pup, all these stars have long periods (433–490 d). And, in any case, inspection of the visual light curves of all six stars on the AAVSO Web site do not show any evidence for dimmings of the magnitude and longevity of those seen in L₂ Pup.

Dimming episodes are seen in symbiotic Miras, where they are attributed to variable dust extinction (Whitelock 1987). A typical dimming at J is 1–2 mag, even larger than that seen in L₂ Pup. We conclude that among non-symbiotic oxygen-rich Miras and semiregulars, the dimming of L₂ Pup appears to be unique.

4 MASS LOSS

Whitelock et al. (2000) noted that L₂ Pup stands out as one of only two low-amplitude SRs with a large $K - [12]$ excess (the other being V CVn), implying a larger mass loss than is usual for SRs. There may be an effect from the low expansion velocity: the dust will remain close to the star longer, thus increasing the $[12]\text{-}\mu\text{m}$ excess.

Stronger evidence for on-going mass loss would come from a $10\text{-}\mu\text{m}$ silicate feature. Such a feature has not been reported, because of the lack of a published 10-micron spectrum. The lack of an original IRAS LRS spectrum is common for bright stars (e.g., α Ceti). However, Volk & Cohen (1989) failed to recover the IRAS spectrum, which seems to have suffered from a technical glitch. ISO did not observe this star.

L₂ Pup was included in the recent survey by the Japanese Infrared Telescope in Space (IRTS) satellite (Murakami et al. 1996). Observations were made using the Mid-Infrared Spectrometer (MIRS) (Roellig et al. 1994; Yamamura et al. 1996), which has

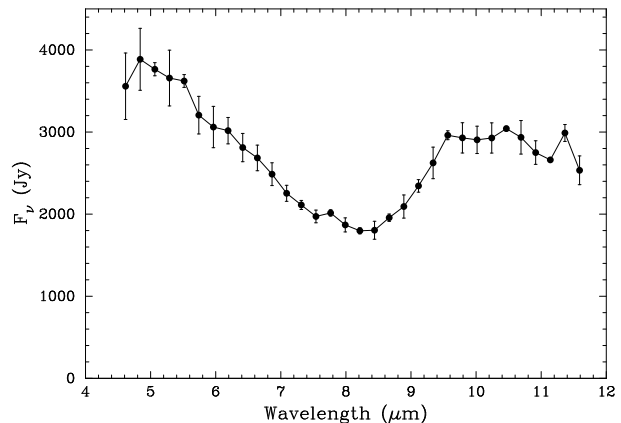


Figure 5. The mid-infrared spectrum taken by the MIRS on board of the Japanese IRTS satellite. Open circles indicate channels affected by glitches. The error bars give the $1\text{-}\sigma$ scatter of the signal in the off source region. Other sources of flux uncertainty, for example, possible change of detector sensitivity, are not included.

an 8×8 arcmin² aperture and scanned with a speed of 4 arcmin/sec. Spectra were taken on 1995 March 30 and April 5, i.e., just before the dimming event. We re-performed the data reduction to correct for effects caused by the high brightness of the star. The coverage in this part of the sky by the IRTS was also below average, resulting in only two well-centred scans over L₂ Pup. The averaged spectrum is shown in Fig. 5.

The spectrum shows a surprisingly strong silicate feature, with a band-to-continuum ratio of about 2.5. This gives a silicate strength parameter (Schutte & Tielens 1989) of $A_{10} = 2.5 \log(F_{\text{obs}}/F_{\text{cont}}) \approx 1$. The continuum between 6 and $8\text{ }\mu\text{m}$ has a slope consistent with the stellar temperature but is brighter than expected from the L -band magnitude of -2.9 .

There is no evidence for a large dust halo around L₂ Pup. We inspected a 4 square degree field in the four IRAS images made using the IRAS Software Telescope (Assendorp et al. 1995): the field shows complicated cirrus structure but no large envelope.

4.1 Mass-loss rate

The silicate feature is very strong compared to the limits on the underlying dust continuum. To quantify this, we fitted the spectrum using the dust model of Siebenmorgen & Kruegel (1992). The model uses as input a blackbody, which we assigned a temperature of $T_{\text{eff}} = 2900\text{ K}$ and luminosity $L_* = 2.0 \times 10^3 L_{\odot}$. The dust was described as a r^{-2} distribution (i.e., constant mass-loss rate) with an inner and outer radius: the mass-loss rate was converted to density assuming an expansion velocity $v_{\text{exp}} = 2.5\text{ km s}^{-1}$. The dust was included as silicate grains with a size distribution $n \propto a^{-3.5}$, with diameter $a > 150\text{ \AA}$. In the fitting procedure, we adjusted the stellar temperature and luminosity, the dust density (or mass-loss rate) and inner radius, to reproduce the MIRS spectrum. The stellar parameters are largely determined by the shorter wavelength observations.

The 25 and $60\text{-}\mu\text{m}$ DIRBE measurements are much higher than the corresponding IRAS values. Part of this can be related to the different response curves: both these DIRBE pass bands cut off a few microns bluer than the IRAS bands. However, the increase over the predicted IRAS flux for the model spectrum is only about 10%. Although the DIRBE beam is much larger than that of IRAS

Table 3. Fitted parameters to the infrared spectrum (1995: pre-dimming) of L_2 Pup, corresponding to the right panel of Fig. 6.

	Model (Jy)	IRAS (Jy)	DIRBE (Jy)	Keck (Jura et al. 2002) (Jy)
$F_{11.7}$	2120			2500
$F_{17.6}$	1810			1700
F_{12}	2100	1990	2137	
F_{25}	1260	783	1385	
F_{60}	127	88	151	
F_{100}	22	27		
Parameters:				
T_{eff}	2900 K			
L_*	$2000 L_{\odot}$			
r_{in}	7.2×10^{14} cm			
r_{out}	1.3×10^{15} cm			
T_{d}^a	350–200 K			
a_{min}	300 Å			
\dot{M}_{d}^b	$5 \times 10^{-10} M_{\odot} \text{ yr}^{-1}$			
\dot{M}_{g}^b	$5.3 \times 10^{-7} M_{\odot} \text{ yr}^{-1}$			

^a range between smallest grains at inner radius and largest grains at outer radius

^b assuming $[\text{Fe}/\text{H}] = -0.7$

(as the telescope was only 19cm, compared to 60cm for IRAS), but there are no other other bright point sources in the beam.

It is difficult to reconcile the photometry with the silicate feature. This is illustrated in Fig. 6, where the left panel shows a fit based the silicate feature, and the right panel shows a fit that includes all photometry. The two models differ in their outer radius, which is smaller for the right panel. The fitted parameters of the right panel (our preferred model) are listed in Table 3. The large number of free parameters means that the fits are not unique: i.e., a larger mass-loss rate with a thinner shell could also fit the spectrum.

The most constraining aspects of the spectrum are the lack of dust emission at $8\mu\text{m}$ and the strong silicate feature, which preclude the presence of hot dust. In our ‘best’ model, the inner radius is at a dust temperature of 350 K, well below the dust condensation temperature. The $17\mu\text{m}$ flux (also dominated by silicate emission) is also surprisingly sensitive to the inner radius and agrees with a dust shell detached from its condensation point. The outer radius is not as well determined as the inner radius. However, a single thin shell can fit the long-wavelength IRAS/DIRBE flux densities. There is no evidence for a cold distant dust shell, consistent with the low CO mass-loss rate found by Olofsson et al. (2002).

Between 4 and $8\mu\text{m}$, the spectral energy distribution indicates a colour temperature consistent with the photospheric temperature. Jura et al. (2002) argued that dust emission dominates from $5\mu\text{m}$, based on evidence that the variability behaviour is very different longward of $5\mu\text{m}$. However, the emission in this band in Mira variables is dominated by water vapour at ~ 2000 K, located in the extended envelope at about 1.5 stellar radii (Matsuura et al. 2002). This water vapour also raises the flux in this region above that extrapolated from the photospheric JHK magnitudes, as seen in the fit. Our findings do not indicate a substantial contribution from dust to the spectrum shortward of $8\mu\text{m}$.

We derive a (pre-dimming) mass-loss rate of $5 \times 10^{-7} M_{\odot} \text{ yr}^{-1}$. This is similar to that estimated by Jura et al. (2002) (post-dimming). They found a dust mass-loss rate 4 times larger than derived by us because they adopted a dust outflow velocity of 10 km s^{-1} rather than 2.5 km s^{-1} , but used a much lower

gas-to-dust ratio, which almost cancels this difference. Our high gas-to-dust ratio is based on the assumption that L_2 Pup is a thick-disk star (see Sec. 4.3), for which we have assumed $[\text{Fe}/\text{H}] = -0.7$. In reality the gas mass-loss rate is not well determined.

4.2 Silicate and Corundum

The model shows that the photometric data imply a narrower silicate feature than is observed. The most likely explanation is that the observed $10\text{-}\mu\text{m}$ feature is not purely silicate. In the scheme of Speck et al. (2000), this feature in L_2 Pup would be classified either as ‘broad’ or possibly as ‘silicate D’. (The difference is subtle and requires continuum subtraction, for which we lack sufficient wavelength coverage.) They fitted the broad feature with a mixture of olivine (MgFeSiO_4) and porous amorphous alumina (or corundum) (Al_2O_3). Corundum has the highest condensation temperature of any circumstellar solid, and is the first condensate to form at $T \approx 1600$ K. Silicates may form subsequently from gas-solid reactions with alumina (Tielens 1990). Hron et al. (1997) suggested that the broad feature is seen in less evolved Mira variables. This may reflect the possibility that, at low \dot{M} , the conversion of alumina to silicate (replacing the Al with Mg) remains incomplete, due to a low reaction rate.

We note that our model calculations used the pre-dimming spectrum. It would be interesting to see whether the spectrum has changed significantly since the dimming. If alumina formed first, the peak of the $10\mu\text{m}$ feature may have shifted to the red. It is tempting to associate the alumina with the grey extinction curve, but it has little extinction in the optical (glass-like). Better candidates would be TiO_2 or pyroxenes (Woitke 1999). The precise agent responsible for the variable polarization also remains undetermined.

4.3 Evolutionary status

Jura et al. (2002) pointed out that the luminosity and effective temperature of L_2 Pup do not unambiguously identify it as an AGB star, and allow the possibility that it is on the first ascent red giant branch. It is not clear whether the spectrum of L_2 Pup shows technetium, which is usually taken as indicating an AGB star. Little et al. (1987) reported a probable detection, while Lebzelter & Hron (1999) listed only a possible detection.

However, if the K -band has significant obscuration then the bolometric magnitude has been underestimated. The bolometric correction would also have been overestimated because of the observed $V - K$ is too large. The two effects combined would mean that the actual luminosity is substantially greater than has been assumed, and is perhaps sufficiently large that placement on the AGB is unambiguous.

Finally, as pointed out by Jura et al. (2002), the space motion of L_2 Pup indicates it may be a thick disk star. Given that the thick disk accounts for up to 13% of the local star density (Chen et al. 2001), it is not unexpected to find a local Mira-like example. If L_2 Pup is indeed a thick-disk star, as seems plausible but which cannot be stated with certainty, the progenitor would likely have had a low metallicity and a low mass.

5 CONCLUSIONS

Visual photometry of L_2 Pup shows an unprecedented dimming over the past 5 years. The long-term light curve shows stable pe-

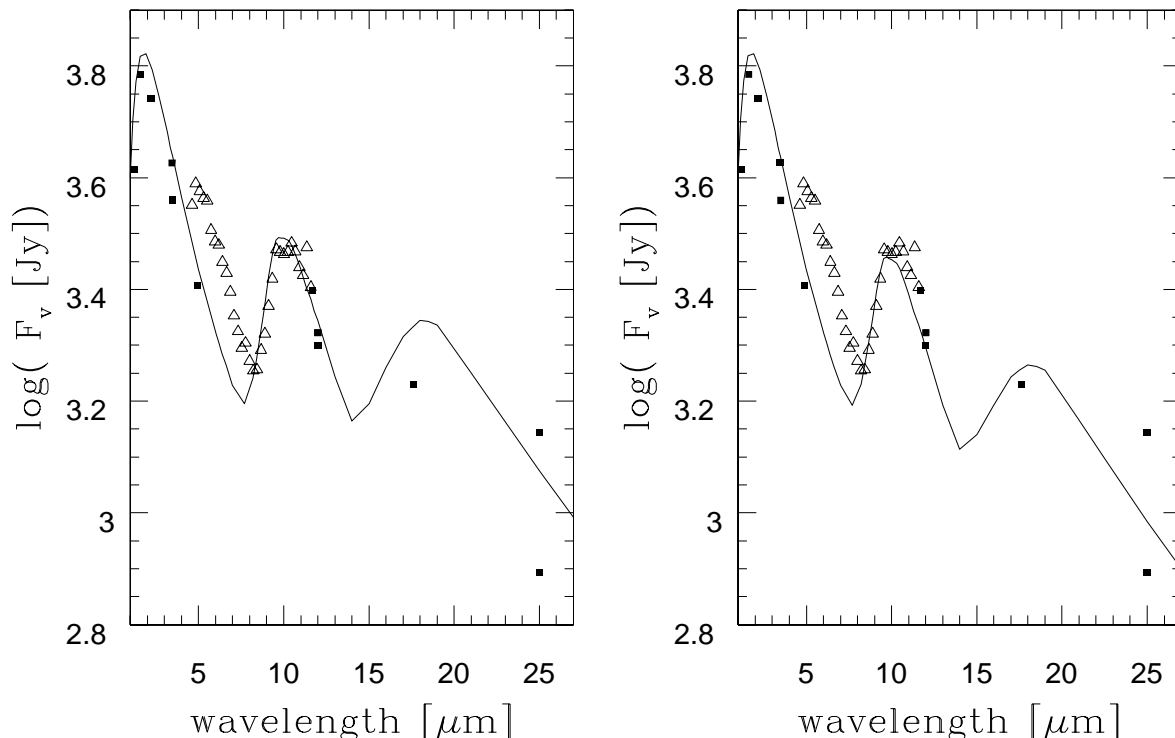


Figure 6. Fit to the MIRS spectrum of L₂ Pup. The MIRS spectrum (1995) is indicated by the open triangles. Filled squares are the average *JHKL* magnitudes, the IRAS 12 and 25 μ m fluxes (1985), the DIRBE 3.5, 4.5, 12 and 25 μ m fluxes (1990), and the 11.7 and 17.6 μ m points (2001) of Jura et al. (2002). Note that the 12 and 25 μ m points refer to very broad bands for which the effective wavelength for this spectral energy distribution is shorter. The left plot shows a fit for the silicate feature. The right plot attempts to better fit the longer-wavelength photometry

riodicity, and we argue that L₂ Pup is Mira-like and should be classified as SRa. The period stability implies a constant stellar radius, which rules out temperature and/or luminosity variations as the cause of the dimming. Rather, the dimming seems to arise from an episode of dust formation close to the extended atmosphere. Episodic dust obscuration events are fairly common in carbon stars but have not been seen in (non-symbiotic) oxygen-rich stars. We suggest that dust forms continuously but anisotropically, with the current dimming event being due to dust formation along the line of sight.

The red colours indicate reddening from dust, but the extinction curve is greyer than found for ISM dust. This could reflect a higher fraction of oxides. The change of colour during the dimming indicates that already before the dimming, the *V*-band magnitude was significantly affected by circumstellar or atmospheric extinction. L₂ Pup was one of the few stars located below the Mira *P-L* relation: the derived *K*-band extinction puts the star in closer agreement with this relation.

We present a 10- μ m spectrum showing strong silicate emission. These observations were carried out in 1995, just prior to the recent dimming. The silicate feature can be fitted with a detached, thin dust shell, with inner radius 7×10^{14} cm and outer radius $\approx 1.5 \times 10^{15}$ cm. Longer wavelength photometry shows no evidence for more distant, colder dust. We derive a mass-loss rate of $\dot{M}_g \approx 5 \times 10^{-7} M_{\odot} \text{ yr}^{-1}$, but this value depends on the assumed expansion velocity and metallicity — if the dust velocity is high, the actual mass-loss rate could be higher.

ACKNOWLEDGMENTS

We are extremely grateful to the observers who have provided visual observations, and to those who have maintained the databases and made them publicly available. We also thank Peter Tuthill for useful discussions. TRB and AR are grateful to the Australian Research Council for financial support.

REFERENCES

- Assendorp, R., Bontekoe, T. R., de Jonge, A. R. W., Kester, D. J. M., Roelfsema, P. R., & Wesselius, P. R., 1995, *A&AS*, 110, 395.
- Bedding, T. R., Kawaler, S. D., Kjeldsen, H., & Zijlstra, A. A., 2002, *MNRAS*. in preparation (Paper II).
- Bedding, T. R., & Zijlstra, A. A., 1998, *MNRAS*, 506, L47.
- Bedding, T. R., Zijlstra, A. A., Jones, A., & Foster, G., 1998, *MNRAS*, 301, 1073.
- Bessell, M. S., Castelli, F., & Plez, B., 1998, *A&A*, 333, 231. Erratum: 337, 321.
- Cannon, A. J., & Pickering, E. C., 1907, *Annals of Harvard College Observatory*, 55, 1.
- Cannon, A. J., & Pickering, E. C., 1909, *Annals of Harvard College Observatory*, 55, 99.
- Cardelli, J. A., Clayton, G. C., & Mathis, J. S., 1989, *ApJ*, 345, 245.
- Chen, B., Stoughton, C., Smith, J. A., Uomoto, A., Pier, J. R., Yanny, B., Ivezić, Ž., York, D. G., Anderson, J. E., Annis, J., Brinkmann, J., Csabai, I., Fukugita, M., Hindsley, R., Lupton, R., Munn, J. A., & the SDSS Collaboration, 2001, *ApJ*, 553, 184.

- Christensen-Dalsgaard, J., Kjeldsen, H., & Mattei, J. A., 2001, *ApJ*, 562, L141.
- Feast, M. W., 1996, *MNRAS*, 278, 11.
- Foster, G., 1996, *AJ*, 112, 1709.
- Henning, T., 1996, In van Dishoeck, E. F., editor, *Proc. IAU Symp. 178, Molecules in Astrophysics: Probes & Processes*, page 343. Dordrecht: Kluwer.
- Houdashelt, M. L., Bell, R. A., Sweigart, A. V., & Wing, R. F., 2000, *AJ*, 119, 1424.
- Hron, J., Aringer, B., & Kerschbaum, F., 1997, *A&A*, 322, 280.
- Jura, M., Chen, C., & Plavchan, P., 2002, *ApJ*, 569, 964.
- Kerschbaum, F., & Olofsson, H., 1999, *A&AS*, 138, 299.
- Kiss, L. L., Szatmáry, K., Cadmus, R. R., & Mattei, J. A., 1999, *A&A*, 346, 542.
- Lebzelter, T., & Hron, J., 1999, *A&A*, 351, 533.
- Little, S. J., Little-Marenin, I. R., & Bauer, W. H., 1987, *AJ*, 94, 981.
- Lloyd Evans, T., 1997, *MNRAS*, 286, 839.
- Magalhaes, A. M., Codina-Landaberry, S. J., Gneiding, C., & Coyne, G. V., 1986, *A&A*, 154, 1.
- Matsuura, M., Yamamura, I., Cami, J., Onaka, T., & Murakami, H., 2002, *A&A*, 383, 972.
- Müller, G., & Hartwig, E. *Geschichte und Literatur der veränderlichen Sterne*, volume Band III. Leipzig: Poeschel & Trepte, 1922.
- Murakami, H., Freund, M. M., Ganga, K., Guo, H., Hirao, T., Hiromoto, N., Kawada, M., Lange, A. E., Makiuti, S., Matsuhara, H., Matsumoto, T., Matsuura, S., Murakami, M., Nakagawa, T., Narita, M., Noda, M., Okuda, H., Okumura, K., Onaka, T., Roellig, T. L., Sato, S., Shibai, H., Smith, B. J., Tanabe, T., Tanaka, M., Watabe, T., Yamamura, I., & Yuen, L., 1996, *PASJ*, 48, L41.
- Olofsson, H., Gonzalez Delgado, D., Kerschbaum, F., & Schoeier, F. L., 2002, *A&A*. accepted.
- Percy, J. R., Colivas, T., Sloan, W. B., & Mattei, J. A., 1990, In Cacciari, C., & Clementini, G., editors, *Confrontation between Stellar Pulsation and Evolution*, volume 11 of *A.S.P. Conf. Ser.*, page 446. San Francisco: ASP.
- Reid, M., & Goldston, J., 2002, *ApJ*. in press astro-ph/0106571.
- Roberts, A. W., 1893, *AJ*, 13, 49.
- Roellig, T. L., Onaka, T., McMahon, T. J., & Tanabe, T., 1994, *ApJ*, 428, 370.
- Schutte, W. A., & Tielens, A. G. G. M., 1989, *ApJ*, 343, 369.
- Siebenmorgen, R., & Kruegel, E., 1992, *A&A*, 259, 614.
- Speck, A. K., Barlow, M. J., Sylvester, R. J., & Hofmeister, A. M., 2000, *A&AS*, 146, 437.
- Szatmáry, K., Gál, J., & Kiss, L. L., 1996, *A&A*, 308, 791.
- Tielens, A. G. G. M., 1990, In Mennessier, M. O., & Omont, A., editors, *From Miras to Planetary Nebulae: Which Path for Stellar Evolution?*, page 186. Gif-sur-Yvette: Editions Frontières.
- van Belle, G. T., Dyck, H. M., Benson, J. A., & Lacasse, M. G., 1996, *AJ*, 112, 2147.
- van Belle, G. T., Thompson, R. R., & Creech-Eakman, M. J., 2002, *AJ*. accepted.
- Vassiliadis, E., & Wood, P. R., 1993, *ApJ*, 413, 641.
- Volk, K., & Cohen, M., 1989, *AJ*, 98, 931.
- Whitelock, P., & Feast, M., 2000, *MNRAS*, 319, 759.
- Whitelock, P., Marang, F., & Feast, M., Dec. 2000, *MNRAS*, 319, 728.
- Whitelock, P. A., 1987, *PASP*, 99, 573.
- Whitelock, P. A., Feast, M. W., Marang, F., & Overbeek, M. D., 1997, *MNRAS*, 288, 512.
- Williams, A. S., 1897, *AJ*, 18, 71.
- Winters, J. M., Le Bertre, T., Jeong, K. S., Helling, C., & Sedlmayr, E., 2000, *A&A*, 361, 641.
- Winters, J. M., Le Bertre, T., Nyman, L.-Å., Omont, A., & Jeong, K. S., 2002, *A&A*, 388, 609.
- Woitke, P., 1999, In Diehl, R., editor, *Astronomy with Radioactivities*, page 163. Garching: Max-Planck-Institut für Extraterrestrische Physik.
- Yamamura, I., Onaka, T., Tanabe, T., Roellig, T. L., & Yuen, L., 1996, *PASJ*, 48, L65.